Paper No.
19071

AMPP ANNUAL CONFERENCE + EXPO
MARCH 19-23, 2023 | DENVER, COLORADO

# Localized corrosion propagation of carbon steel in inhibited environment: a potentiostatic approach

Bernardo Santos
Institute for Corrosion and Multiphase Technology
Ohio University
342 West State St, Athens, OH 45701
USA

Marc Singer
Institute for Corrosion and Multiphase Technology
Ohio University
342 West State St, Athens, OH 45701
USA

Maria Serenario
Institute for Corrosion and Multiphase Technology
Ohio University
342 West State St, Athens, OH 45701
USA

Maalek Mohamed-Said
TotalEnergies
OneTech - CSTJF, Avenue Larribau
F-64018 Pau
France

Xi Wang
Institute for Corrosion and Multiphase Technology
Ohio University
342 West State St, Athens, OH 45701
USA

Alysson Helton Santos Bueno
CESTEq – Center of Surface Engineering, Tribology and Electrochemistry
Federal University of Sao Joao del Rei
170 Frei Orlando Square, Sao Joao del Rei
36307352
Brazil

David Young
Institute for Corrosion and Multiphase Technology
Ohio University
342 West State St, Athens, OH 45701
USA

## ABSTRACT

The initiation of carbon steel localized corrosion is commonly observed in inhibited environments, both in field and laboratory settings, even though the uniform corrosion rate remains low. While many reasons have been reported to explain pit initiation, little research has considered whether these pits will propagate or not. This work focuses on evaluating the tendency of localized corrosion propagation due to galvanic coupling between the inhibited surface and active pit. Complexity in simulating this phenomenon likely influences the paucity of research addressing this mechanism. Given that its main

driving force is the difference in potential between both surfaces, the potentiostatic technique is an interesting methodology to simulate this corrosion mechanism. This work was done considering a primarily imidazolinium-based corrosion inhibitor under produced water conditions (5 wt.% NaCl, pH 4.5, $CO_2$) at 55 and 80°C. Linear polarization resistance (LPR) and potentiodynamic polarization were used to obtain baseline results and characterize the inhibitor performance. The baseline anodic potentiodynamic sweeps indicated that, at certain critical anodic potential/current conditions, the inhibitor is fully desorbed from the surface. Several potentiostatic experiments were conducted, maintaining the electrode potential in between the open circuit potential and this critical desorption potential – this was meant to simulate, albeit very artificially, different levels of galvanic couple that could exist in case of active localized corrosion and to investigate why active corrosion could still persist inside a pit even though the corrosion inhibitor was still present in the bulk solution. It is acknowledged that this methodology makes this work quite exploratory and that the results should be viewed as preliminary. The potentiostatic experiments indicated that, at certain anodic potentials, the injection of inhibitor did not decrease the current measured to the same levels expected from the baseline potentiodynamic sweeps. Increased inhibitor dosage proved to be necessary at certain conditions to significantly decrease the current. However, at high current levels, further injections were insufficient, indicating that substrate dissolution might undermine the adsorption of the inhibitor.

Key words: Corrosion inhibition, Localized corrosion propagation, Inhibition efficiency, Imidazoline, High temperature, Potentiostatic.

## INTRODUCTION

Localized corrosion is known as the most dangerous and unpredictable corrosion mechanisms found in hydrocarbon production and transmission systems. This mode of corrosion has the potential to cause serious financial loss, environmental damage, production interruption, and even loss of life. Over the years, corrosion engineers have made significant improvements on prediction and mitigation techniques to extend the lifespan of carbon steel pipelines, such as using of corrosion inhibitors; injection of such chemicals has proven to be effective and economic, making them a first choice over other alternatives. However, long-term use of organic corrosion inhibitors in the oil and gas industry has shown a high potential for occurrence of localized attack. This might take place when the inhibitor is not appropriate to the operating conditions or when the inhibitor dosage is too low, in the presence of corrosion product layers or sand, or when the pipeline surface is exposed to extreme shear stress [1,2]. Although pit initiation has been widely reported in the presence of inhibitors[1,3,4], discussion of propagation has been limited.

The propagation process is typically driven by the local galvanic coupling established between the area covered by the corrosion products or corrosion inhibitors and the bare steel surface area of the pit. Galvanic current drives the propagation of the pit causing severe damage to exposed metal surfaces. Some authors [5–7] attempted to simulate this mechanism using cells composed of two electrodes – a cathode and an anode – in which they had their surface properly prepared to act as such and then were connected via a zero-resistance ammeter (ZRA) to monitor the galvanic current. The separation between the electrodes giving rise to ohmic resistance was one of the challenges faced by the authors[7]. The poor understanding of the involved phenomena stems from the complex system that does not lend itself to artificial simulation. Thus, it is important to develop methodologies that aim to simulate the mechanisms involved.

While the ZRA setup mentioned above is the “gold standard” when investigating galvanic coupling, other, less complicated, techniques can be used to give some insights on the phenomena. The potentiostatic methodology emerges as an interesting rapid and easy alternative to simulate artificially such phenomenon using only one working electrode in a conventional three-electrode electrochemical cell. Once a potential is applied to the working electrode, a current will be induced. One should be able to apply different ranges of potential to the artificial anode simulating the propagation of localized corrosion might take place following the aforementioned model. Therefore, if the inhibitor is efficient, one should observe a decrease on the current flowing through the sample when injecting the corrosion inhibitor into

the solution. The methodology would also allow a better understanding of the electrochemical parameters that govern the adsorption/desorption mechanisms of the inhibitors as well as improving the existing models[8] for this matter. Consequently, the objective of this work is to utilize the potentiostatic methodology to further understand the role of inhibitor and important factors in stifle the propagation of localized corrosion of carbon steel. The next step of this work will be to design a proper ZRA setup and repeat this study.

## EXPERIMENTAL PROCEDURE

Carbon steel C1018 (UNS G10180[(1)]) was machined into flat specimens and mounted in epoxy for the electrochemical experiments. The chemical composition of the material used is listed in Table 1. The ferritic and pearlitic microstructure contained 2.28 wt.% of cementite phase ($Fe_3C$) according to the lever rule. The surface was grinded with #180, and #400 grit silicon carbide abrasive paper with water flow, finished with #600 grit SiC abrasive paper with isopropanol flow, cleaned in an ultrasonic isopropanol bath and air-dried prior to each experiment.

**Table 1: Composition (wt.%) of flat C1018 carbon steel specimens.**

| Element | C | Al | Cu | Mn | Mo | Ni | S | Si | Fe |
|---|---|---|---|---|---|---|---|---|---|
| Composition | 0.16 | 0.007 | 0.088 | 0.65 | 0.019 | 0.055 | 0.010 | 0.25 | Balance |

All experiments were performed using a 2 L glass cell. The electrolyte was an aqueous solution with 5 wt.% NaCl, $CO_2$ as sparging gas, 1 bar total pressure and pH 4.5. Temperatures of 55°C and 80°C were assessed. Prior to each experiment, the electrolyte was sparged with $CO_2$ for at least 2 hours to deoxygenate; sparging was continuous during each experiment to avoid any oxygen ingress and maintain $CO_2$ saturation. The pH of the solution was maintained at 4.5 ± 0.1 by adding hydrochloric acid (HCl) and sodium bicarbonate ($NaHCO_3$). The corrosion inhibitor used in this study is an imidazolinium-based commercial inhibitor in the concentration of 50 ppm. This dosage is the recommended by the manufacturer and it is above the surface saturation concentration (SSC) for both temperatures.

A three-electrode electrochemical cell was used having a Pt-coated mesh as counter electrode, a KCl saturated Ag/AgCl reference electrode (connected to the glass cell *via* a salt bridge and a Luggin capillary), and the C1018 as the working electrode. The electrochemical measurements were conducted using a potentiostat. Open circuit potential (OCP), electrochemical impedance spectroscopy (EIS) and linear polarization resistance (LPR) measurements were taken. The EIS data was collected at OCP from 5 kHz to 1 Hz with a perturbation amplitude of 10 mV rms. The LPR measurements were conducted using a range from -5 mV to +5 mV vs. OCP, with a scan rate of 0.125 mV/s using a B value of 26 mV for corrosion rates calculations. At the conclusion of each experiment, a cathodic potentiodynamic sweep was conducted. The anodic potentiodynamic sweep was conducted after the OCP returned to the original value before the cathodic sweep.

### Baseline experiments

Establishing baselines of uninhibited and fully inhibited bare steel prior to the potentiostatic experiments is essential to understand the potential and current densities ranges in which the material will respond whenever a potential is applied. In this step, the corrosion rates were monitored using LPR for 5 hours

[(1)] UNS numbers are listed in *Metals and Alloys in the Unified Numbering System*, published by the Society of Automotive Engineers (SAE International) and cosponsored by ASTM International.

under the inhibited and uninhibited conditions. For the inhibited environment, the inhibitor was injected into the solution after 20 minutes of pre-corrosion. For both conditions, after assessing the corrosion rate evolution, potentiodynamic sweeps took place cathodically and anodically.

### Potentiostatic experiments

At this stage, before applying any potential to the sample, the sample stayed in the solution for OCP stabilization for 20 minutes. The working electrode was then polarized to 4 different positive fixed potentials over the OCP of the bare steel ($mV_{OCP,\ bare\ steel}$), simulating possible scenarios:

- +25 $mV_{OCP,\ bare\ steel}$ – to simulate the localized corrosion propagation when there is a galvanic coupling established between a surface covered with iron carbonate ($FeCO_3$) and the active surface of the pit (bare surface) [6].
- +70 $mV_{OCP,\ bare\ steel}$ – to simulate the localized corrosion propagation when there is a more severe galvanic coupling established between the surface covered with corrosion inhibitors and the active surface of the pit.
- +100 $mV_{OCP,\ bare\ steel}$ – to simulate a more extreme condition in which the difference in potential is higher than the OCP difference between the area covered and the area uncovered with inhibitor.
- +150 $mV_{OCP,\ bare\ steel}$ – to apply an overpotential in the sample close to the desorption potential [9] observed in the baseline tests.

For all potentiostatic tests, the potential was applied to the sample in an uninhibited environment (5 wt.% NaCl, pH 4.5, $CO_2$) for 300 seconds (5 minutes), and then 50 ppm of the corrosion inhibitor was injected into the solution. The induced current was monitored throughout the experiment, and additional dosage of the inhibitor was added when necessary.

## RESULTS

### Baseline experiments

The corrosion rate (from LPR) changes over time for both inhibited (CI) and uninhibited (bare steel) environments at 55°C and 80°C are depicted in Figure 1. For the bare steel conditions the rates did not appreciably change, although the condition at 80°C was slightly more aggressive with corrosion rates of around 3 mm/year after 5 hours. As expected, with injection of the corrosion inhibitor the corrosion rates dropped significantly for both temperatures, with the 55°C condition yielding values as low as 0.1 mm/year after 5 hours. Even so, it must be highlighted that at 80°C there was a residual corrosion rate above 0.1 mm/y after 5 hours of experiment.

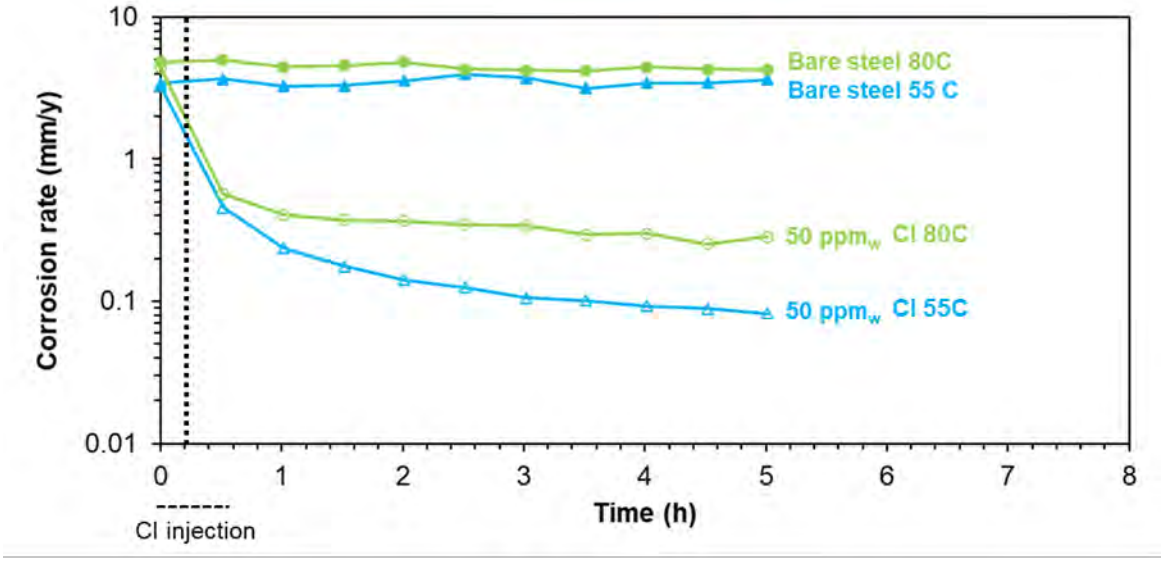


**Figure 1: LPR corrosion rates over time for inhibited and uninhibited condition at 55 and 80°C.**

The main purpose of this section is to document the anodic current one should expect during the potentiostatic tests. The anodic potentiodynamic sweeps were performed in all four conditions (55°C and 80°C and with/without inhibitor), and the curves are shown in Figure 2.

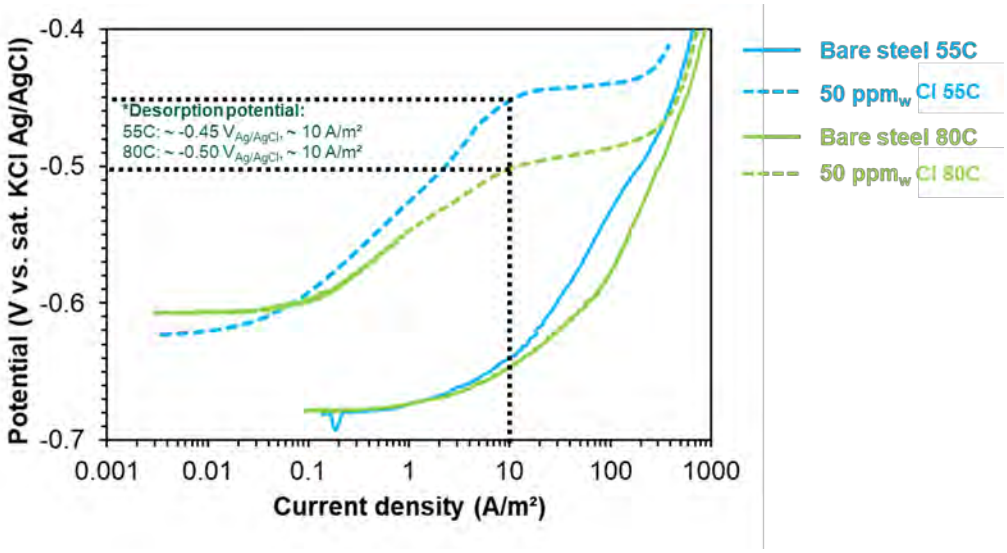


**Figure 2: Baseline anodic sweeps for the inhibited and non-inhibited condition at 55 and 80°C.**

In the uninhibited environment, the anodic sweeps obtained at both temperatures behaved similarly, with the one at 55°C being slightly retarded in comparison to the one at 80°C. Temperature also played a negative role in the inhibited environment as the curve associated to 80°C was slightly accelerated in relation to that observed at 55°C. Another important observation relates to the so-called "desorption potential" [9–11] for the anodic sweep in the inhibited condition. According to the literature, it is assumed that the inhibitor adsorbed on the steel surface would be fully or partially desorbed when the potential is applied above a certain critical anodic potential. The main reason for this behavior is linked to a phenomenon called electrochemical desorption[12], associated to the Langmuir isothermal model[8], that states that applying an anodic potential generates an electrostatic repulsion between the surface and the inhibitor that weakens the adsorption bond. At this point the current increases rapidly and the material starts to behave like bare steel again, evidenced by the overlapping of the curves in both environments

over *ca.* 450 $mV_{Ag/AgCl}$ as shown in Figure 2. Although different desorption potentials were observed for both temperatures, the desorption current seemed to be similar (Figure 2), suggesting that the current density on the specimen might be the main parameter that affected the adsorption and desorption process in this scenario.

**Potentiostatic experiments**

The methodology is to compare the potential/current response observed before and after the inhibitor injection on the polarized sample. This should give some clues on whether or not the addition of inhibitor can stifle higher anodic currents caused by polarization (simulating how a anodic site on the steel, subject to galvanic coupling, behaves with the addition of inhibitor).

+25 $mV_{OCP,\ bare\ steel}$

Figure 3 shows anodic polarization scans indicating the range of current densities (e.g., about 5 $A/m^2$ at 55°C for bare steel) one should expect when applying +25 $mV_{OCP,\ bare\ steel}$ to the sample. After the addition of corrosion inhibitor, the current density should move from values regarding the bare steel (left plot), to the values shown for the inhibited anodic sweep (right plot). According to the figure, for this fixed potential, negative currents should be observed when the inhibitor is injected, since the fixed potential lies on the cathodic side of the inhibited baseline potentiodynamic sweep.

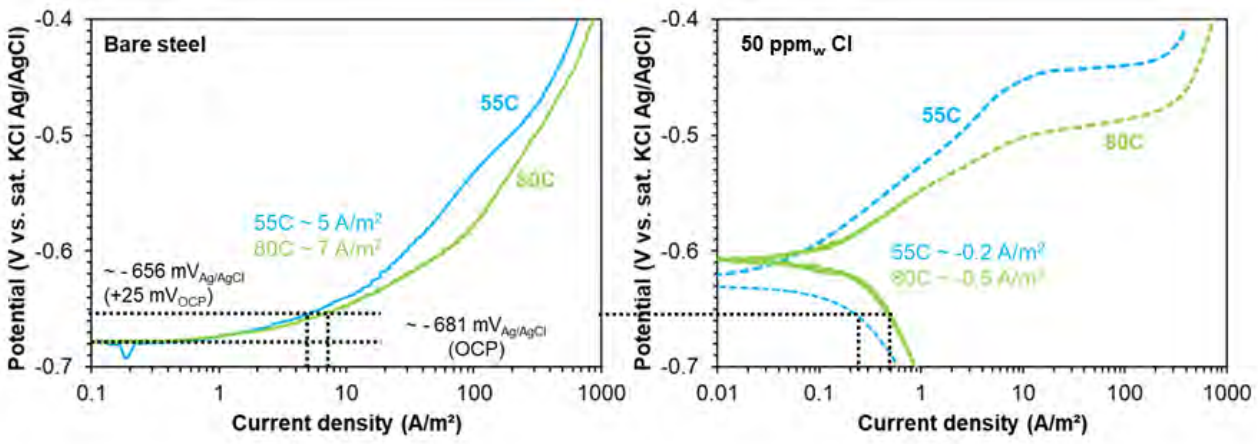


**Figure 3: Anodic polarization curves showing the current density expected for bare steel (left) and inhibited environment (right) during +25 $mV_{OCP,\ bare\ steel}$ potentiostatic experiment. Condition: 5 wt.% NaCl, $CO_2$, pH 4.5, 50 ppm corrosion inhibitor (CI).**

Figure 4 shows the current densities during the +25 $mV_{OCP,\ bare\ steel}$ potentiostatic experiment for both 55°C and 80°C. During the initial and uninhibited 300 seconds, the current densities were stable, even though at 80°C it decreased slightly before the corrosion inhibitor injection. Immediately after the injection of the inhibitor, the current dropped significantly for both temperatures, taking less than 200 seconds to reach negative values, as expected from the baseline curves shown in Figure 2. After 2000 seconds both currents levelled-off in a negative range indicating that full adsorption of the inhibitor occurred, and the measured currents were in agreement with the baseline tests.

The increase in the corrosion potential of bare steel caused by the inhibitor adsorption was greater than the applied potential (intrinsic potential difference due to surface condition difference). Translating these results to a real scenario, there was a role reversal, and the “anode” (actively corroding pit) started now acting as the cathode favoring the cathodic reaction and limiting the rate of the anodic dissolution. The

measured net current was consequently negative since it was representative of the cathodic reaction. This is obviously not a good example of active pitting but is shown here for academic purposes.

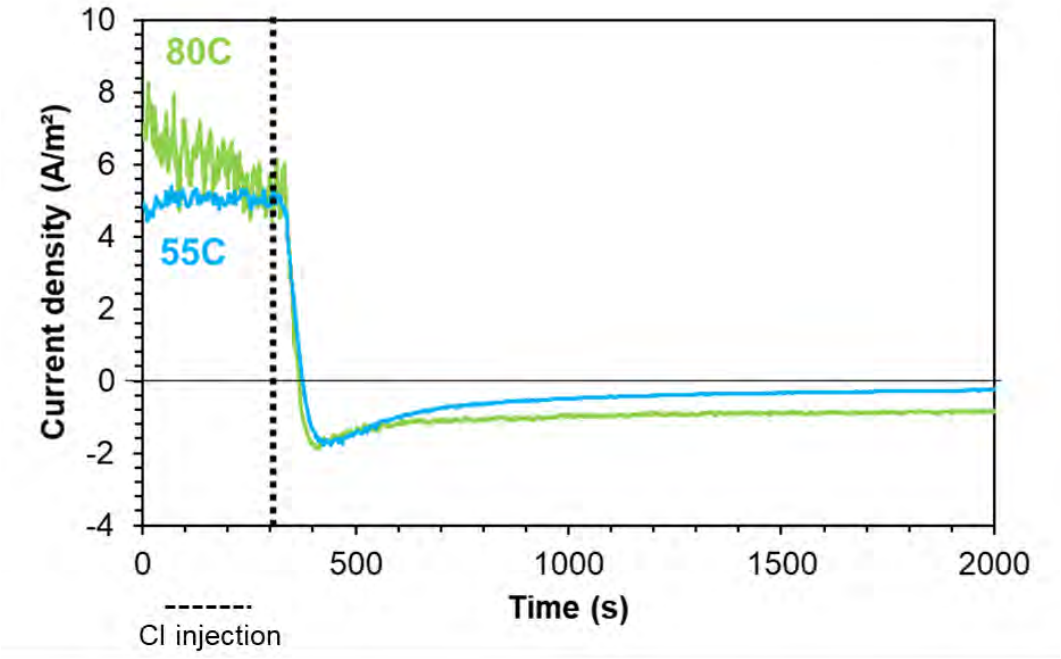


**Figure 4: Net current density over time for +25 $mV_{OCP,\ bare\ steel}$ potentiostatic experiment. Condition: 5 wt.% NaCl, $CO_2$, pH 4.5, 50 ppm corrosion inhibitor (CI) added after 300 seconds.**

+70 $mV_{OCP,\ bare\ steel}$

Figure 5 shows anodic polarization scans indicating the baseline current densities expected for the +70 $mV_{OCP,\ bare\ steel}$ potentiostatic experiment. This scenario aimed to simulate localized corrosion propagation when the substrate lacked inhibitor coverage. The applied potential in Figure 6 is close to the measured OCP in the inhibited environment (Figure 5), hence the current densities should stabilize around 0 $A/m^2$ for both temperatures.

Figure 6 shows that higher temperatures lead to higher initial current densities during the 300 second uninhibited period. If converted to corrosion rates, the initial metal dissolution was in the order of 26.9 and 36.1 mm/y for 55°C and 80°C, respectively. After injection of the inhibitor both current densities dropped as expected. Both conditions stabilized the net current density at a very low level close to the ones extracted from the baseline curves shown in Figure 5. Therefore, this applied potential was not high enough to hinder the adsorption of the inhibitor, meaning that the dissolution of the substrate did not undermine adsorption of the inhibitor molecules on the specimen surface.

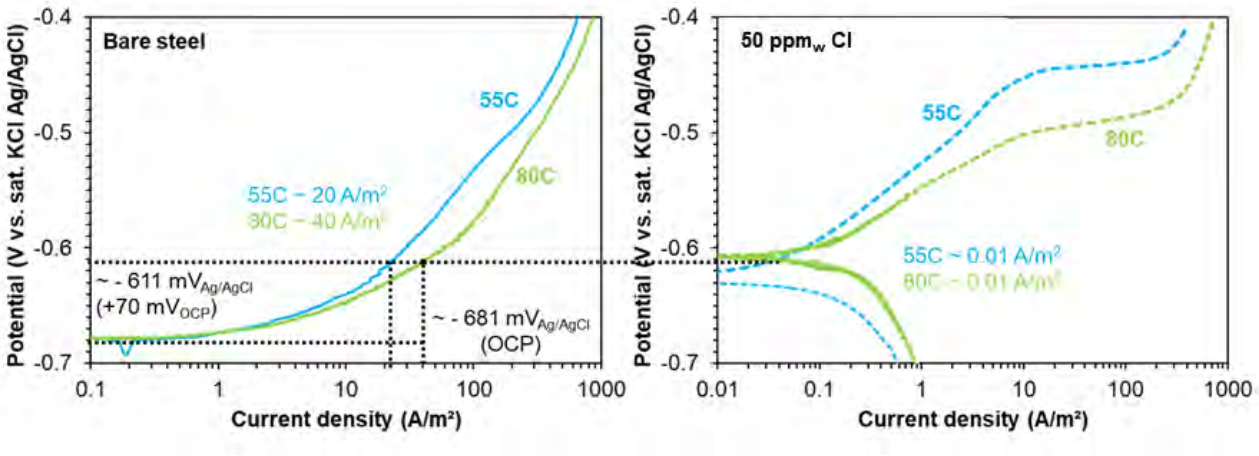


**Figure 5: Anodic polarization curves showing current density expected for bare steel (left) and inhibited environment (right) during +70 $mV_{OCP,\ bare\ steel}$ potentiostatic experiment. Condition: 5 wt.% NaCl, $CO_2$, pH 4.5, 50 ppm corrosion inhibitor (CI).**

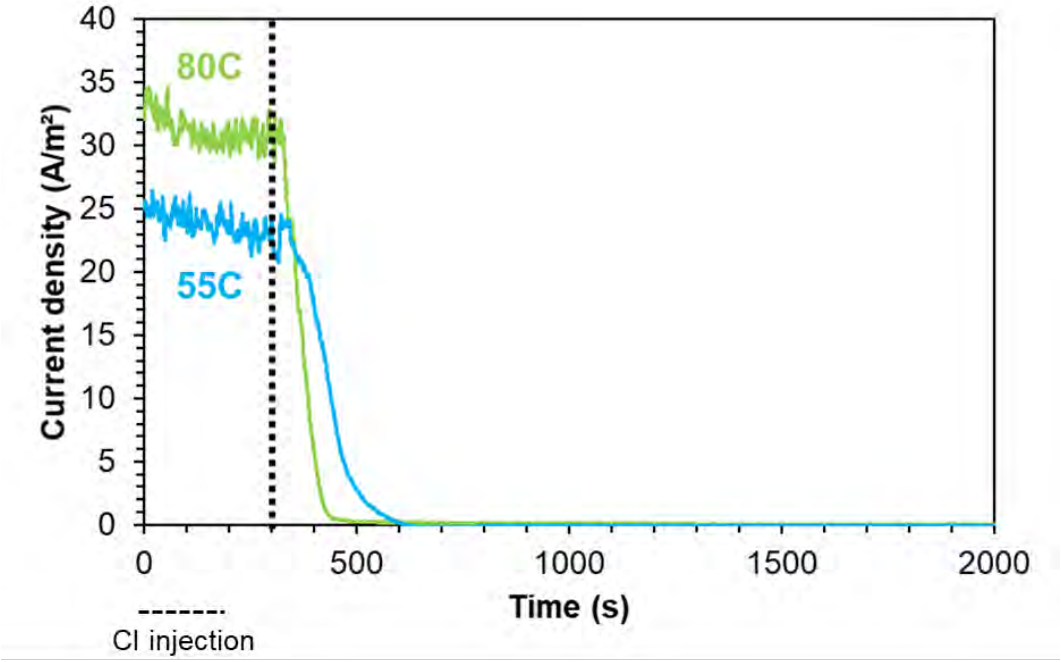


**Figure 6: Current density over time for +70 $mV_{OCP,\ bare\ steel}$ potentiostatic experiment. Condition: 5 wt.% NaCl, $CO_2$, pH 4.5, 50 ppm corrosion inhibitor (CI) added after 300 seconds.**

+100 $mV_{OCP,\ bare\ steel}$

Figure 7 shows anodic polarization scans indicating the baseline current densities expected for the +100 $mV_{OCP,\ bare\ steel}$ potentiostatic experiment. Considering the inhibited environment, although the applied potential was higher than the OCPs of inhibited conditions, the resulting inhibited current densities should still be significantly lower than the one for the uninhibited condition.

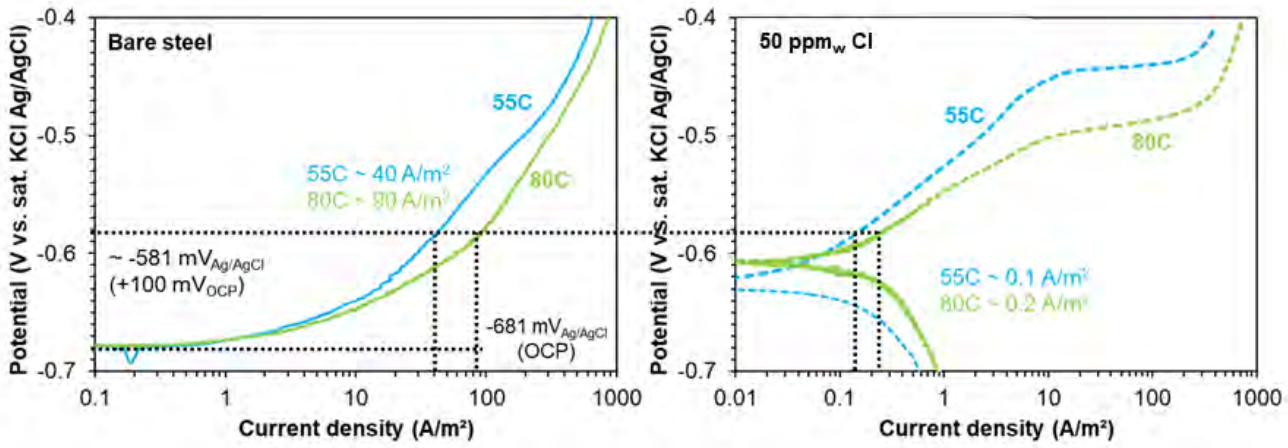


**Figure 7: Anodic polarization curves showing current density expected for bare steel (left) and inhibited environment (right) during +100 $mV_{OCP,\ bare\ steel}$ potentiostatic experiment. Condition: 5 wt.% NaCl, $CO_2$, pH 4.5, 50 ppm corrosion inhibitor (CI).**

Figure 8 shows that the current densities decreased for both temperatures after the inhibitor injection. However, instead of levelling-off at a very low value, around 0.1-0.2 A/m$^2$ as indicated in Figure 7, after the initial decrease the current densities increased and stabilized at a higher value than that expected, *ca.* 7.2 A/m$^2$ at 55 °C and *ca.* 26.4 A/m$^2$ at 80 °C. The potential range between the OCP of the inhibited condition and the desorption potential can be considered as an unstable region for the inhibitor on the surface. Although the inhibitor is able to adsorb on the surface, as seen from the initial decrease after the inhibitor injection, the measured current dominated by the dissolution of the substrate is high enough to render the surface lack of full coverage by inhibitor molecules. In other words, the higher the potential applied from the OCP of the uninhibited environment, the harder it is for the inhibitor to adsorb and to stifle the dissolution of the substrate.

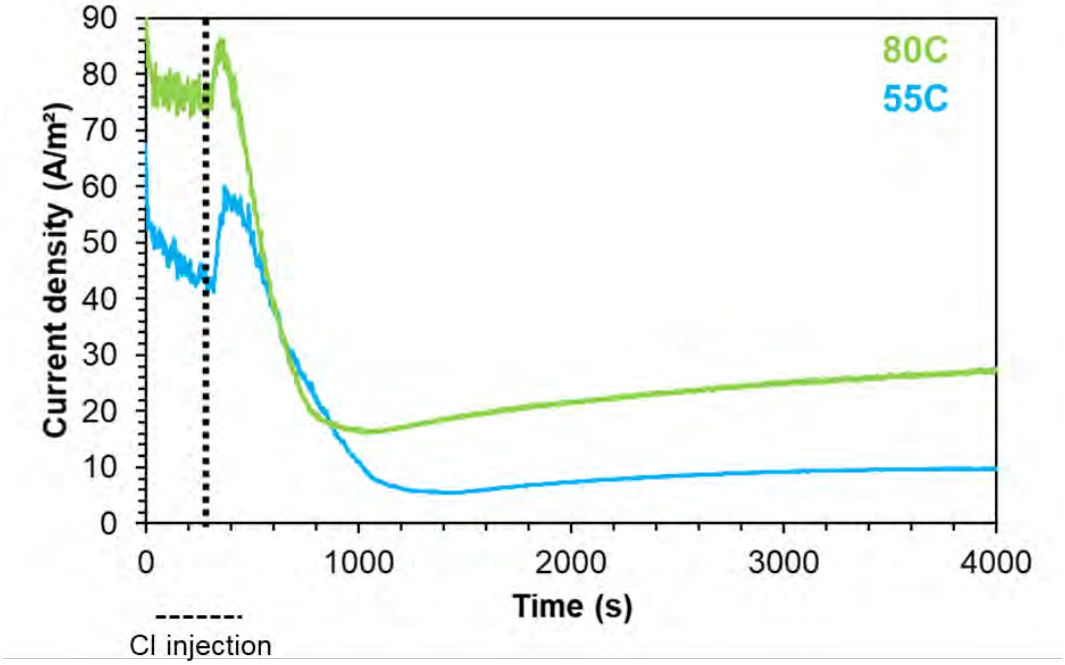


**Figure 8: Current density over time for +100 $mV_{OCP,\ bare\ steel}$ potentiostatic experiment. Condition: 5 wt.% NaCl, $CO_2$, pH 4.5, 50 ppm corrosion inhibitor (CI) added after 300 seconds.**

Since the current densities were stabilized at a relatively high values, extra injections of corrosion inhibitor were conducted to examine if further inhibition could be induced, as shown in Figure 9. With the subsequent drop in current after the second inhibitor injection, there is clearly a dosage dependency on the corrosion inhibition of a polarized surface. The main reason for that might regards on the depletion of bulk CI concentration in a closed system bringing the need of extra dosages. However, for the higher temperature, even after 15000 seconds (*ca.* 4 hours) the current densities were still high at *ca.* 2.91 A/m$^2$. At the end of tests, the corrosion rates would be 0.05 mm/y at 55 °C and 3.13 mm/y at 80 °C converted from current densities per ASTM-G102 [13].

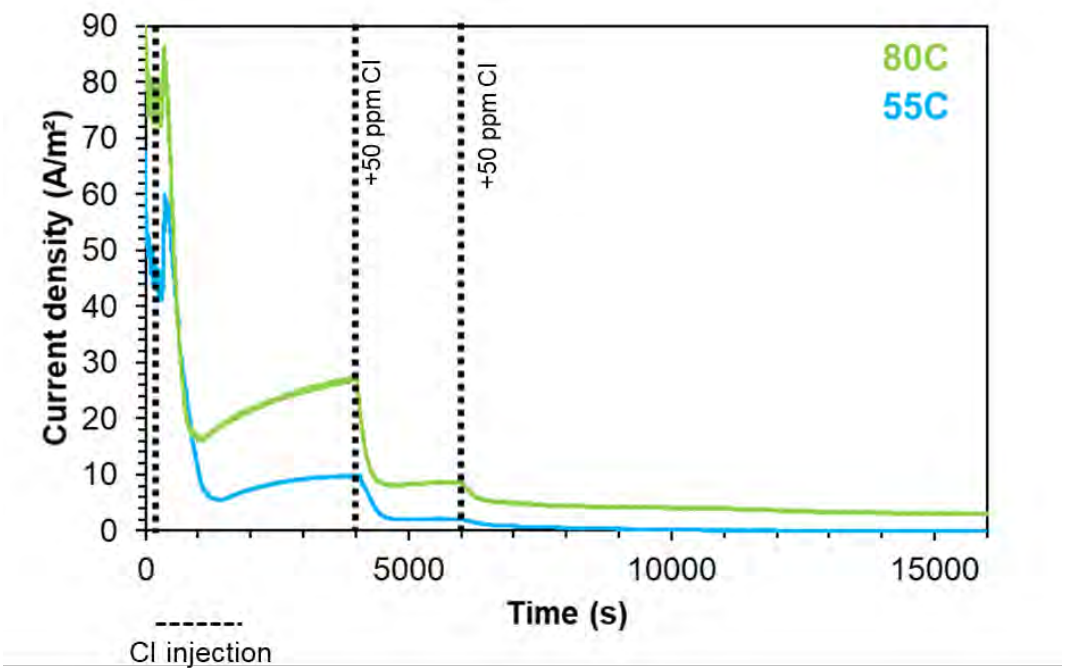


**Figure 9: Continuation of the +100 $mV_{OCP, bare\ steel}$ potentiostatic experiment. Condition: 5 wt.% NaCl, $CO_2$, pH 4.5, with 2 additional dosages of 50 ppm corrosion inhibitor (CI) added at different times.**

+150 $mV_{OCP, bare\ steel}$

Figure 10 shows anodic polarization scans indicating the ranges of current densities expected for the +150 $mV_{OCP, bare\ steel}$ potentiostatic experiment. Even though this potential lies closer to the "desorption potential" determined from the polarization curves, the current density should decrease at least 2 orders of magnitude according to the baseline polarization curve if the inhibitor is efficient.

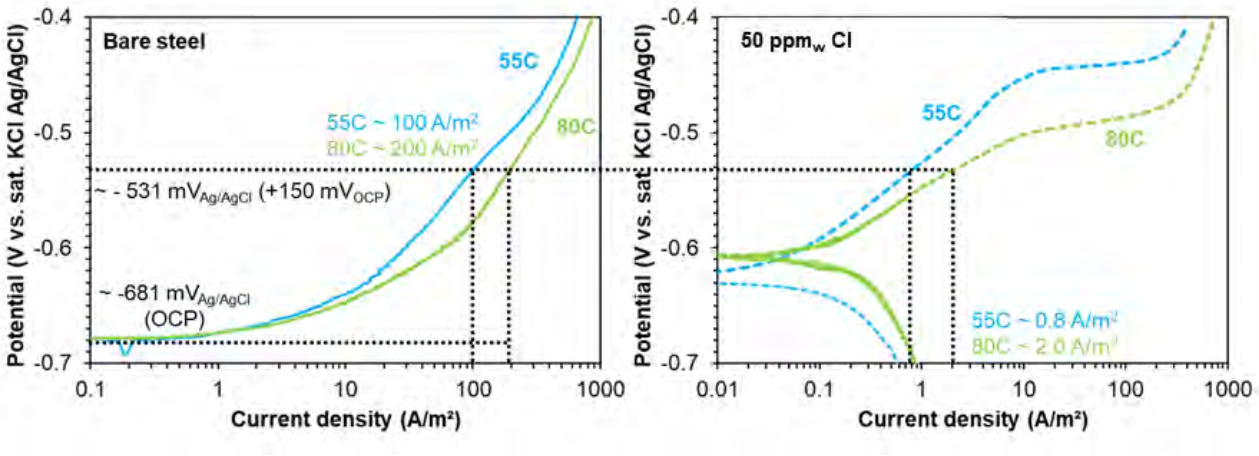


**Figure 10: Anodic polarization curves showing current density expected for bare steel (left) and inhibited environment (right) during +150 $mV_{OCP,\ bare\ steel}$ potentiostatic experiment. Condition: 5 wt.% NaCl, $CO_2$, pH 4.5, 50 ppm corrosion inhibitor (CI).**

Figure 11 shows that the current densities increased compared to the initial 300 seconds of the uninhibited environment after the corrosion inhibitor injection. In the instability potential range, it can be assumed that the closer it approaches to the "desorption potential", the harder for the inhibitor to adsorb on the polarized surface, since the iron dissolution is more vigorous.

Extra dosages of inhibitor were added to the solution for both temperatures after the corrosion rates stabilized. At 80°C, although the current density showed a slight decrease after each injection, the effect was cancelled out since the current started increasing again shortly. At this point, the dissolution of the substrate was very likely undermining the inhibitor adsorption on the surface, no matter the concentration of the corrosion inhibitor in the solution.

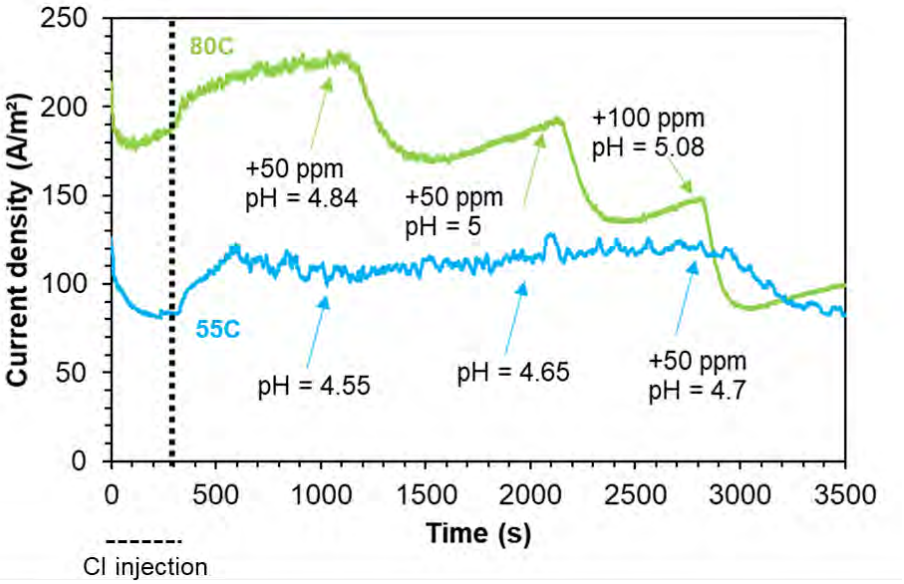


**Figure 11: Current density over time for +150 $mV_{OCP,\ bare\ steel}$ potentiostatic experiment. Condition: 5 wt.% NaCl, $CO_2$, pH 4.5, several dosages of corrosion inhibitor (CI) were added at different times.**

Before elucidating the reason why the inhibitor failed at potentials close to but still lower than the "desorption potential", it is important to highlight that the high amount of cementite (2.28%) presented in the C1018 microstructure can play a significant role on hindering the inhibition. In such microstructure, the ferrite tends to be consumed preferentially over the cementite[14,15]. Therefore, as the material corrodes, the cementite network will be revealed on the surface, increasing the material exposed area. It is also known that the thicker the cementite layer is, the more unlikely it is to observe a good inhibition, since there will be an increase on the cathodic area [16]. Thus, in this present work, the higher the applied potential is in the uninhibited environment, the thicker the cementite layer exposed should be, and hence the lower the inhibition effect is.

In this matter, considering the parameters of this set of experiments (sample being polarized during inhibitor adsorption), an adjusted potentiodynamic anodic sweep was plotted to be compared with the baseline one shown in Figure 2. Various potentials were selected (the 4 potentials showed previously included) to be applied to the sample using the same aforementioned procedure (50 ppm of inhibitor injected only after 300 s) in the same environment, at 55°C. Then, when the current density reached a steady-state value, this value was recorded and used to plot an adjusted anodic sweep for the inhibitor under the polarizing condition, shown in Figure 12. It is important to stress that the adjusted curve is created by the addition of several points, and it was not obtained in the traditional way.

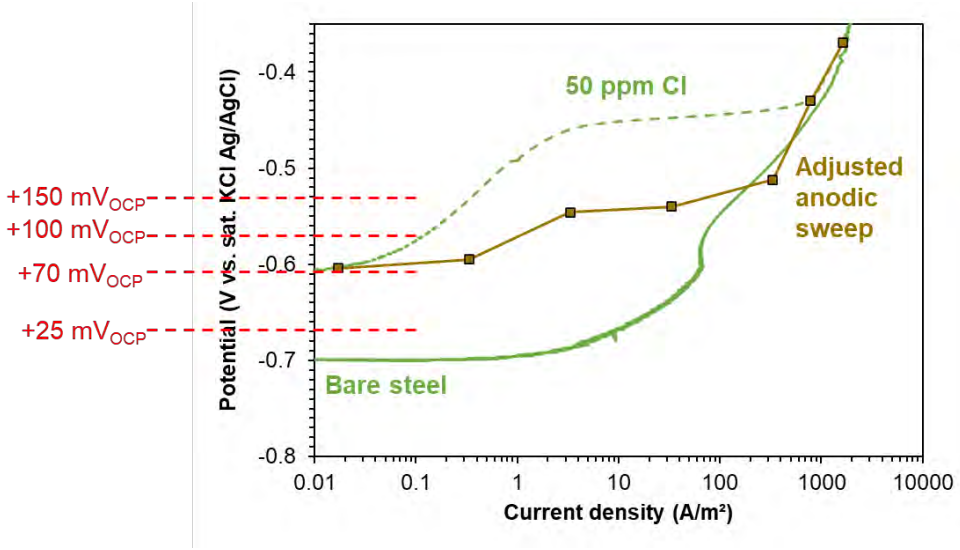


**Figure 12: Adjusted anodic sweep for inhibited environment considering sample being polarized. Condition: 5 wt.% NaCl, $CO_2$, pH 4.5, 55°C, 50 ppm corrosion inhibitor (CI).**

The kinetics shown by the adjusted anodic sweep is significantly accelerated compared to the baseline inhibited curve (50 ppm CI on a freshly polished surface). The same inhibition behavior should not be expected from the inhibitor on a propagating localized corrosion site. For instance, the +150 $mV_{OCP,\ bare\ steel}$ lies in the region (Figure 12) where the material already started behaving as the bare steel again, which indicates that the inhibitor adsorption on the surface is suppressed, and the current density values for +100 $mV_{OCP,\ bare\ steel}$ are now closer to what was observed previously in Figure 8.

It is necessary to highlight that there are other electrochemical components less discussed in the work that might be playing a role behind the failure of the inhibitor under these conditions. Although this may not be the best method to elucidate the trend, the adjustment of the curve gives an idea of how the cementite network is affecting the inhibition negatively. The following factors are anticipated as detrimental due to experimental artefact, that need further investigations:

- The CI concentration in the bulk can be depleted because tests were conducted in close system with one shot CI injection.
- The screened cases considered configuration where first the surface is polarized and then CI is injected. The cases where a film is first established and then the anodic polarization is applied should complement herein findings.
- Other commercial CI should be tested as the ability to limit localized corrosion propagation depends upon the type of CI.
- All the tests are conducted under “artificially” imposed current to mimic “localized corrosion propagation configuration”. There is ongoing work to simulate the same configuration but with real galvanic set-up and various anode/cathode surface ratio.

## CONCLUSIONS

The following conclusions can be drawn from the above results:

- The ability of the corrosion inhibitor to adsorb on the polarized sample depends on the magnitude of the current density flowing on the sample surface.

- At overpotentials closer to the desorption potential in inhibited solution, extra amounts of CI are needed to stifle the anodic dissolution and decrease the net current density to values as low as the ones observed in the baseline experiments.

- The methodology addresses only the effects on the anode of a simulated galvanic coupling. Further effects on the cathode played by the injection of inhibitor could also be considered using an actual galvanic coupling setup i.e., using two electrodes acting as anode and cathode.

## ACKNOWLEDGEMENTS

This project has been supported by TotalEnergies. The authors would like to thank TotalEnergies for their financial support and valuable discussions. The authors would also like to thank both the Brazilian National Council of Technological and Scientific Development - CNPq for (200454/2020-0 and 405505/2021-3) and The Minas Gerais Research Funding Foundation – Fapemig (APQ-02540-21) for their financial support in this work.

## REFERENCES

1. F. Farelas, M. Singer, D. Nugraha, S. Whitehurst, B. Kinsella. "Localized corrosion in the presence of corrosion inhibitors at high flow velocities in CO2 Environments". NACE - International Corrosion Conference Series. 2018;2018-April(11269):1-14.
2. W. Li, B.F.M. Pots, B. Brown, K.E. Kee, S. Nesic. "A direct measurement of wall shear stress in multiphase flow-Is it an important parameter in CO2 corrosion of carbon steel pipelines?" *Corros Sci*. (2016);110:35-45.
3. C.S. Brossia, G.A. Cragnolino. "Effect of environmental variables on localized corrosion of carbon steel", *Corrosion*. (2000);56(5):505-514.
4. G.A. Schmitt, W. Bucken, R. Fanebust. "Modeling Microturbulences At Surface Imperfections As Related To Flow-Induced Localized Corrosion", *Corrosion*. (1992);48(5):431-440.

5. J. Marsh, J.W. Palmer, R.C. Newman. "Evaluation of inhibitor performance for protection against localized corrosion", NACE - International Corrosion Conference Series. Vol 2002-April. ; 2002.
6. J. Han. "Galvanic Mechanism of Localized Corrosion for Mild Steel in Carbon Dioxide Environments" Ohio University, Thesis, (2009).
7. A. Turnbull, D. Coleman, A.J.Griffiths, P.E. Francis, L. Orkney. "Effectiveness of corrosion inhibitors in retarding propagation of localised corrosion". NACE - International Corrosion Conference Series. 2002;2002-April(02274):1-14.
8. H. Swenson, N.P. Stadie. "Langmuir's Theory of Adsorption: A Centennial Review", *Langmuir*. (2019).
9. M.A. Pletnev. "Effect of inhibitors on the desorption potentials in the anodic dissolution of iron in acid solutions – A review", *Int J Corros Scale Inhib*. (2020);9(3):842-866.
10. W.J. Lorenz, F. Mansfeld. "Interface and interphase corrosion inhibition", *Electrochim Acta*. (1986);31(4):467-476.
11. X. Zhang, F. Wang, Y. He, Y. Du. "Study of the inhibition mechanism of imidazoline amide on CO2 corrosion of Armco iron", *Corros Sci*. (2001);43(8):1417-1431.
12. V.J. Drazic, D.M. Drazic. "Influence of the metal dissolution rate on the anion and inhibitor adsorption", 7th European Symposium on Corrosion Inhibitors (7SEIC)1990.
13. ASTM G102. "Standard Practice for from Electrochemical Measurements". *Astm*. 2015;89(Reapproved 2015):1-7.
14. R.C. Souza, B.A.F. Santos, M.C. Gonçalves, et al. "The role of temperature and H2S (thiosulfate) on the corrosion products of API X65 carbon steel exposed to sweet environment", *J Pet Sci Eng*. (2019);180:78-88.
15. B.A.F. Santos, M.E.D. Serenario, R.C. Souza, et al. "The electrolyte renewal effect on the corrosion mechanisms of API X65 carbon steel under sweet and sour environments", *J Pet Sci Eng*. (2021);199108347.
16. A.A. Al-Asadi. "Iron Carbide Development and its Effect on Inhibitor Performance" Ohio Univeristy, Thesis, (2014)